Structural Engineering and Mechanics, Vol. 31, No. 2 (2009) 137-152
DOI: http://dx.doi.org/10.12989/sem.2009.31.2.137

Theoretical analysis of Y-shape bridge and application

Lu Peng-zhen†

School of Civil Engineering, Southwest Jiaotong University, Chengdu 610031, China

Zhang Jun-ping‡

School of Civil Engineering of Guangzhou University, Guangzhou 510006, China

Zhao Ren-da‡†

School of Civil Engineering, Southwest Jiaotong University, Chengdu 610031, China

Huang Hai-yun‡‡

School of Civil Engineering of Guangzhou University, Guangzhou 510006, China

(Received January 5, 2007, Accepted December 4, 2008)

Abstract. Mechanic behavior of Y-shape thin-walled box girder bridge structure is complex, so one can not exactly hold the mechanical behavior of the Y-shape thin-walled box girder bridge structure through general calculation theory and analytical method. To hold the mechanical behavior better, based on elementary beam theory, by increasing the degree of freedom analytical method, taking account of restrained torsiondistortion angledistortion warp and shearing lag effect at the same time, authors obtain a thin-walled box beam analytical element of 10 degrees of freedom of every node, derive stiffness matrix of the element, and code a finite element procedure. In addition, authors combine the obtained procedure with spatial grillage analytical method, meanwhile, they build a new analytical method that is the spatial thin-walled box girder element grillage analysis method. In order to validate the precision of the obtained analysis method, authors analyze a type Y-shape thin-walled box girder bridge structure according to the elementary beam theory analytical method, the shell theory analytical method and the spatial thin-walled box girder element grillage analysis method respectively. At last, authors test a type Y-shape thin-walled box girder bridge structure. Comparisons of the results of theory analysis with the experimental text show that the spatial thin-walled box girder element grillage analysis method is simple and exact. The research results are helpful for the knowledge of the mechanics property of these Y-shape thin-walled box girder bridge structures.

Keywords: structure of Y-shape bridge; increasing of freedom degree; stiffness matrix; space grillage analysis.

† Postgraduate, Corresponding author, E-mail: pzh_lu@163.com, lupengzhen2008@hotmail.com
‡ Professor, E-mail: zhangjp168@163.com
‡† Professor, E-mail: rendazhao@163.com
‡‡ Lecturer, E-mail: luyule5588@163.com

1. Introduction

Y-shape bridge structure is an effective way to solve the problem of traffic congestion in modern cities. To solve the traffic congestion problem, a great number of the Y-shape bridges were built in different regions. Cross-section form of the Y-shape bridge structure mainly adopts the box girder structure. With the increasing of the use of the thin-walled box girder structure, the mechanic behavior of the Y-shape bridge structure becomes more complicated, especially in strained torsiondistortion angledistortion warp and shearing lag effect. Scholars at home and abroad Huang (1994), Ding (1996), Li and Pi (1996), Hambly (1982), Morreu *et al.* (1996), Mira Mitra *et al.* (2004), Thuc Phuong Vo and Lee (2006) and so on have studied the design and structural analysis method about the Y-shape bridge structure based on the theory of the thin-walled box girder.

The disposal method of the structure in the past mainly can be expressed as follows. Firstly, the Y-shape bridge structure was generally divided into two independent structures, then the two independent structures were analyzed respectively. This method can not take account into interaction between main bridges and ramps. Secondly, the analysis of the Y-shape bridge structure was carried out according to the elementary beam theory, this method can not take account of the restrained torsionthe distortion anglethe distortion warp and the shearing lag effect. Thirdly, the analysis of Y-shape bridge structure adopts the shell theory, this method can not obtain directly internal force, and the workload of post-process is heavy. In a word, the above mentioned methods can not exactly deal with the structural mechanical behavior, what's worse, they may lead to insecurity of structural design.

Based on the above theory, by increasing degree of freedom analytical method, taking account of the strained torsionthe distortion anglethe distortion warp and the shear lag effect at the same time, authors obtain the thin-walled box beam analytical element of 10 degrees of freedom of every node, derive stiffness matrix of the element, and code a finite element procedure. In addition, authors combine the obtained procedure with the spatial grillage analytical method, and build a new analytical method that is the spatial thin-walled box girder element grillage analysis method. In order to validate the precision of the obtained analysis method, authors analyze the typical Y-shape thin-walled box girder bridge structure according to the elementary beam theory analytical method, the shell theory analytical method and the spatial thin-walled box girder element grillage analysis method respectively. At the same time, authors test the typical Y-shape thin-walled box girder bridge structure. Comparisons of results of theory analysis with experimental text show that the spatial thin-walled box girder element grillage analysis method is simple and exact. The research results offer a new method to solve the complicated mechanical behavior of the Y-shape thin-walled box girder bridge structures.

2. Element stiffness analysis of Y-shape bridge straight girder

2.1 Stiffness analysis of restrained torsion of thin-walled straight box girder

2.1.1 Nodal displacement of element and choice of nodal force

Element of the thin-walled straight box girder that authors built is shown in Fig. 1. Vectors of the nodal force of the thin-walled box girder element under element coordinate system adopt $\{\bar{F}\}$, and

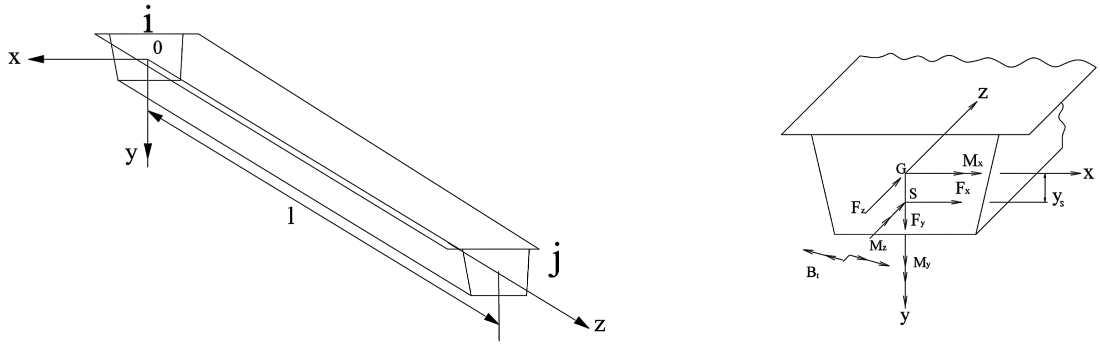

Fig. 1 System of coordinates and nodal force in thin-walled box straight girder element

vectors of the element displacement adopts $\{\overline{\delta}\}$.

$$\{\overline{F}\} = [F_{xi}, F_{yi}, N_{zi}, M_{xi}, M_{yi}, M_{zi}, B_{Ii}, M_{\zeta i}, M_{Di}, B_{Di}, F_{xj}, F_{yj}, N_{zj}, M_{xj}, M_{yj}, M_{zj}, B_{Ij}, M_{\zeta j}, M_{Dj}, B_{Dj}]^T \quad (1)$$

$$\{\overline{\delta}\} = [u_i, v_i, w_i, \theta_{xi}, \theta_{yi}, \theta_{zi}, f_i, \zeta_i, r_i, r_i', u_j, v_j, w_j, \theta_{xj}, \theta_{yj}, \theta_{zj}, f_j, \zeta_j, r_j, r_j']^T \quad (2)$$

2.1.2 Differential equation of the restrained torsion

Solutions of the restrained torsion basic equation of the closed cross-section beam are presented by the minimal theorem of potential energy.

$$\theta_z(z) = A_1 z + A_2 z + A_3 e^{-kz} + A_4 e^{kz} - \frac{m_z}{2GK} z^2 \qquad f(z) = A_2 - \frac{k}{\mu} A_3 e^{-kz} + \frac{k}{\mu} A_4 e^{kz} - \frac{m_z}{GK} z \quad (3)$$

2.1.3 Element stiffness matrix taking account of the restrained torsion

The element stiffness matrix $[K]$ of the thin-walled straight box girder taking account of the restrained torsion can be divided into four subsidiary matrixes, as shown in formula (4), stiffness equation of buckling and torsion of the element is expressed according to the order of the freedom degree $\{\delta\}$ of the node displacement, as shown in Eq. (5) (Huang and Xie 2000), force factors of the cross-section torque and buckling bimoment of constraint force can be shown in Eq. (6).

$$[K] = \begin{bmatrix} K_{I,I} & K_{I,J} \\ K_{J,I} & K_{J,J} \end{bmatrix} \quad (4)$$

$$\begin{bmatrix} K_{6,6} & K_{6,7} & K_{6,16} & K_{6,17} \\ K_{7,6} & K_{7,7} & K_{7,16} & K_{7,17} \\ K_{16,6} & K_{16,7} & K_{16,16} & K_{16,17} \\ K_{17,6} & K_{17,7} & K_{17,16} & K_{17,17} \end{bmatrix} \begin{Bmatrix} \theta_{zi} \\ f_i \\ \theta_{zj} \\ f_j \end{Bmatrix} = \begin{Bmatrix} M_{zi} \\ B_{Ii} \\ M_{zj} \\ B_{Ij} \end{Bmatrix} \quad (5)$$

$$M_z = \frac{1}{\mu} E' I_\omega \theta_z''' - GK\theta_z' \qquad B_I = -E' I_\omega f' \quad (6)$$

2.1.4 Equivalent nodal force

Equivalent node load of the thin-walled box girder under uniformly distribute loading are presented as follows.

$$\overline{M}_{zi} = \overline{M}_{zj} = -\frac{1}{2}m_z l, \quad \overline{B}_{Ii} = -\overline{B}_{Ij} = \frac{m_z}{T_1}\left[0.5l^2(chkl+1) - \frac{ul}{k}shkl\right] - \frac{\mu}{k^2}m_z \tag{7}$$

In the formulas (7): $T_1 = 2 - 2chkl + \frac{kl}{\mu}shkl$

2.1.5 Cross-section stress analysis

Vertical normal stress and buckling normal stress of cross-section are expressed as follows in turn.

$$\sigma = \left(\frac{N}{A_G} + \frac{M_x}{I_x}y - \frac{M_y}{I_y}x\right) - \frac{B_I}{I_\omega}\hat{\omega}_n \qquad \sigma_\omega = -\frac{B_I}{I_\omega}\hat{\omega}_n \tag{8}$$

2.2 Distortion stiffness analysis of the thin-walled straight box girder

2.2.1 Basic differential equation of eistortion

$$\gamma_D^{(4)} + 4\lambda^4\gamma_D = \frac{m_d}{E'I_{\omega D}} \tag{9}$$

In the Eq. (9), $\lambda = \sqrt[4]{I_R/4I_{\omega D}}$ is an attenuation coefficient of the box girder cross-section distortion deformation.

2.2.2 Element stiffness matrix taking account of distortion deformation

Distortion stiffness equation of the straight girder element adopts matrix form, as shown in formula (10), the element stiffness coefficients of the formula (10) can be obtained on the basis of definition of the stiffness coefficient and the regulation which takes account of the positive direction of the constraint force, as illustrated in Eq. (11). In the Eq. (11), when degree of freedom $\gamma_{Di}, \gamma'_{Di}, \gamma_{Dj}, \gamma'_{Dj}$ brings about unit displacement respectively, subscript m adopts 9, 10, 19 and 20 respectively.

$$\begin{bmatrix} K_{9,9} & K_{9,10} & K_{9,19} & K_{9,20} \\ K_{10,9} & K_{10,10} & K_{10,19} & K_{10,20} \\ K_{19,9} & K_{19,10} & K_{19,19} & K_{19,20} \\ K_{20,9} & K_{20,10} & K_{20,19} & K_{20,20} \end{bmatrix} \begin{Bmatrix} \gamma_{Di} \\ \gamma'_{Di} \\ \gamma_{Dj} \\ \gamma'_{Dj} \end{Bmatrix} = \begin{Bmatrix} M_{Di} \\ B_{Di} \\ M_{Dj} \\ B_{Dj} \end{Bmatrix} \tag{10}$$

$$\begin{aligned} K_{9,m} &= M_{Di} = E'I_{\omega D}\gamma_D'''(0) & K_{19,m} &= M_{Dj} = -E'I_{\omega D}\gamma_D'''(\lambda l_s) \\ K_{10,m} &= B_{Di} = -E'I_{\omega D}\gamma_D''(0) & K_{20,m} &= B_{Dj} = E'I_{\omega D}\gamma_D''(\lambda l_s) \end{aligned} \tag{11}$$

2.2.3 Calculation of distortion moment

According to literature (Huang and Xie 2000), eccentric loading in the girder can always be divided into normal symmetrical loading and unsymmetrical loading, as shown in Fig. 2. The unsymmetrical loading becomes torsion loading, and the torsion loading can be again divided into

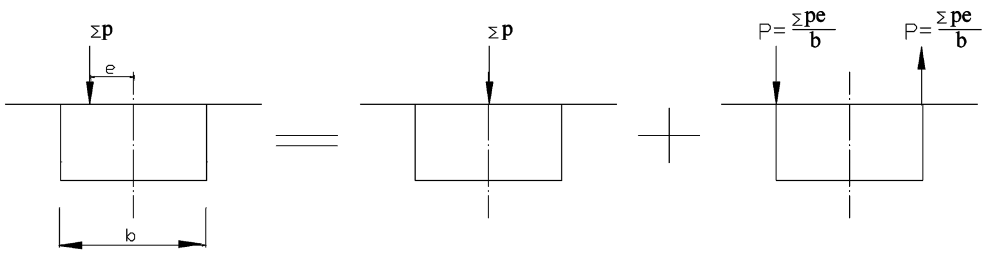

Fig. 2 Decomposition of eccentric load

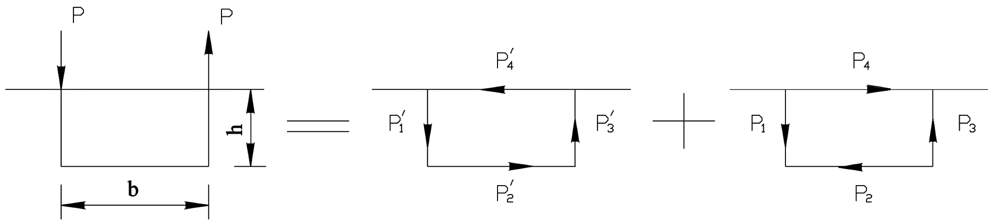

Fig. 3 Decomposition of torsion load

pure torsion loading and distortion loading of mutual balance, as shown in Fig. 3.

In accordance with the definition of shearing force flow, rigid torsion loading $P'_1 \sim P'_4$ and distortion loading $P_1 \sim P_4$ can be presented as follows.

$$P'_1 = P'_3 = \frac{\Sigma Pe}{2b}, \quad P'_2 = P'_4 = \frac{\Sigma Pe}{2h}, \quad P_1 = P_3 = \frac{\Sigma Pe}{2b}, \quad P_2 = P_4 = \frac{\Sigma Pe}{2h} \tag{12}$$

Then torque and distortion moment is expressed as follows.

$$M_t = P_1 b + P_2 h = \Sigma Pe \qquad M_D = \frac{1}{2}P_1 b + \frac{1}{2}P_2 h = \frac{1}{2}\Sigma Pe \tag{13}$$

2.2.4 Distortion equivalent nodal force

According to the literature (Huang and Xie 2000), when one puts the distortion loading on the girder, equivalent distortion moment and equivalent distortion bimoment of two end node can be received:

1) Uniformly distribute distortion moment m_D on the girder

$$\overline{M}_{Di} = \overline{M}_{Dj} = -\frac{m_D[ch(\lambda l_s) - \cos(\lambda l_s)]}{\lambda T_2} \qquad \overline{B}_{Di} = -\overline{B}_{Dj} = \frac{m_D[sh(\lambda l_s) - \sin(\lambda l_s)]}{2\lambda^2 T_2} \tag{14}$$

2) Concentrated distortion moment M_D on the span middle cross-section

$$\overline{M}_{Di} = \overline{M}_{Dj} = \frac{M_D}{T_2}\left(sh\frac{\lambda l_s}{2}\cos\frac{\lambda l_s}{2} + ch\frac{\lambda l_s}{2}\sin\frac{\lambda l_s}{2}\right) \qquad \overline{B}_{Di} = \overline{B}_{Dj} = \frac{M_D}{\lambda T_2}sh\frac{\lambda l_s}{2}\sin\frac{\lambda l_s}{2} \tag{15}$$

In the Eq. (15): $T_2 = sh(\lambda l_s) + \sin(\lambda l_s)$

2.2.5 Distortion stress analysis of cross-section

Distortion normal stress of any point on the cross-section can be obtained directly through the distortion bimoment B_D of the cross-section.

$$\sigma_D = -\frac{B_D}{I_{\omega D}}\omega_{Dn}$$

2.3 Stiffness analysis of shearing force lag effect of the thin-walled straight box girder

2.3.1 Basic differential equation of the shearing force lag

$$\begin{aligned} E'I_y u_s^4 = q_x \qquad & E'I_x v_s^4 - E'I_{y\zeta}\zeta''' = q_y \\ E'Aw''_G + E'S_\zeta\zeta'' = -qz \qquad & E'I_\zeta\zeta'' + E'S_\zeta w''_G + E'I_{y\zeta}v'''_s - GK_\zeta\zeta = 0 \end{aligned} \tag{16}$$

2.3.2 Element stiffness matrix taking account of shearing force lag deformation

The shearing force lag stiffness equation adopts matrix form as follow.

$$\begin{bmatrix} K_{1,1} & \cdots & K_{1,6} & K_{1,11} & \cdots & K_{1,16} \\ \vdots & \ddots & \vdots & \vdots & \ddots & \vdots \\ K_{6,1} & \cdots & K_{6,6} & K_{6,11} & \cdots & K_{6,16} \\ K_{11,1} & \cdots & K_{11,6} & K_{11,11} & \cdots & K_{11,16} \\ \vdots & \ddots & \vdots & \vdots & \ddots & \vdots \\ K_{16,1} & \cdots & K_{16,6} & K_{16,11} & \cdots & K_{16,16} \end{bmatrix} \{u\}^e = \{F\}^e \tag{17}$$

In the Eq. (17)

$$\begin{aligned} \{F\}^e &= [F_{Xi}, F_{yi}, N_i, M_{xi}, M_{yi}, M_{\zeta i}, F_{Xj}, F_{yj}, N_j, M_{xj}, M_{yj}, M_{\zeta j}] \\ \{u\}^e &= [u_i, v_i, w_i, \theta_{xi}, \theta_{yi}, \theta_{zi}, f_i, \zeta_i, r_i, r'_i, u_j, v_j, w_j, \theta_{xj}, \theta_{yj}, \theta_{zj}, f_j, \zeta_j, r_j, r'_j]^T \end{aligned} \tag{18}$$

Because flexure deformation on *xoz* plane and on the *yoz* plane of the straight girder uncouple, the flexure deformation on *xoz* plane and on the *yoz* plane can be calculated respectively. Degrees of freedom 1, 5, 11, 15 of the element flexure stiffness equation on the *xoz* are expressed according to plane girder theory

$$EI_y \begin{bmatrix} \frac{12}{l^3} & \frac{6}{l^2} & -\frac{12}{l^3} & \frac{6}{l^2} \\ \frac{6}{l^2} & \frac{4}{l} & -\frac{6}{l^2} & \frac{2}{l} \\ -\frac{12}{l^3} & -\frac{6}{l^2} & \frac{12}{l^3} & \frac{6}{l^2} \\ \frac{6}{l^2} & \frac{2}{l} & -\frac{6}{l^2} & \frac{4}{l} \end{bmatrix}^e \begin{Bmatrix} u_{si} \\ \theta_{yi} \\ u_{sj} \\ \theta_{yj} \end{Bmatrix}^e = \begin{Bmatrix} F_{xi} \\ M_{yi} \\ F_{xj} \\ M_{yi} \end{Bmatrix}^e \tag{19}$$

The element deformation stiffness in the *yoz* plane can be presented according to the definition of the stiffness coefficient. When the degree of freedom $v_i, w_i, \theta_{xi}, \zeta_i, v_j, w_j, \theta_{xj}, \zeta_j$ bring about unit displacement in turn, the subscript m of the stiffness coefficient $K_{2,m}, K_{3,m}, K_{4,m}, K_{8,m}$ and $K_{12,m}, K_{13,m}, K_{14,m}, K_{18,m}$ of the formula (19) adopt 2, 3, 4, 8 and 12, 13, 14, 18 respectively.

2.3.3 Equivalent node force of shearing force lag

Calculation method of equivalent node force is similar to the stiffness coefficient, solution of the equivalent node force can be presented through the basic differential equation, and the corresponding solution of the freedom degree of the basic differential equation can be obtained under the uniformly distribute loading of the "*y*" and "*x*" axes directory. Then the equivalent node force is presented on the basis of boundary condition as follows.

$$\begin{aligned}
&\overline{F}_{yj} = E'I_x v''' - E'I_{y\zeta}\zeta''\big|_{z=l} && \overline{F}_{yi} = E'I_x v''' - E'I_{y\zeta}\zeta''\big|_{z=0} \\
&\overline{N}_j = -E'A'\omega'_G - E'S_\zeta\zeta'\big|_{z=l} && \overline{N}_i = -E'A'\omega'_G - E'S_\zeta\zeta'\big|_{z=0} \\
&\overline{M}_{xj} = -E'I_x v'' + E'I_{y\zeta}\zeta'\big|_{z=l} && \overline{M}_{xi} = -E'I_x v'' + E'I_{y\zeta}\zeta'\big|_{z=0} \\
&\overline{M}_{\zeta j} = -E'I_\zeta\zeta' - E'S_\zeta\omega' + E'I_{y\zeta}v''\big|_{z=l} && \overline{M}_{\zeta i} = -E'I_\zeta\zeta' - E'S_\zeta\omega' + E'I_{y\zeta}v''\big|_{z=0}
\end{aligned} \tag{20}$$

The results of solution above taking account of shearing force lag effect can be presented by the corresponding procedure, and normal stress is obtained at last.

2.3.4 Element stiffness of the thin-walled straight girder taking account of the shearing force lag, the restrained torsion and the distortion

According to the characteristic of the straight box girder structure and the mechanic behavior, under external loading, the torque, the moment and the distortion and others uncouple, so the restrained torsion, the distortion and the shearing force lag taking account of the stiffness calculation respectively. Then each result of the stiffness calculation is combined. Therefore, after taking account of the restrained torsionthe distortion anglethe distortion warp and the shearing force lag effect based on elementary girder theory, authors obtain a thin-walled straight box girder analytical element stiffness matrix $[K]_{20\times 20}$ of 10 degrees of freedom of every node. In order to shorten this paper, only the element stiffness matrix $[K_{I,I}]$ is shown in Eq. (21). In the Eq. (21)

$$K_{6,6} = -K_{6,16} = K_{16,16};\ K_{6,7} = K_{6,17} = \frac{K_{7,16}}{k} = -K_{16,17};\ K_{7,7} = -K_{17,17};\ K_{9,9} = K_{19,19};\ K_{9,10} = -K_{19,20}$$

$$K_{9,20} = -K_{10,19};\ K_{10,10} = K_{20,20};\ K_{10,20} = \frac{2E'I_{\omega D}\lambda^3}{p}[ch(\lambda l)\sin(\lambda l) - \sin(\lambda l)\cos(\lambda l)];$$

$$K_{7,17} = \frac{GK\mu(-kl + \mu shkl)}{2\mu k(1 - chkl) + klshkl};\ K_{9,19} = \frac{4E'I_{\omega D}\lambda^3}{p}[ch(\lambda l)\sin(\lambda l) + sh(\lambda l)\cos(\lambda l)]$$

$$\mu = 1 - \frac{K}{I_p},\ k = \sqrt{\frac{\mu GK}{E'I_\omega}},\ p = sh^2(\lambda l) - \sin^2(\lambda l)$$

$$\begin{bmatrix} EI_y\frac{12}{l^3} & 0 & 0 & 0 & EI_y\frac{6}{l^2} & 0 & 0 & 0 & 0 & 0 \\ 0 & EI_x\frac{12}{l^3} & 0 & -EI_x\frac{6}{l^2} & 0 & 0 & 0 & 0 & 0 & 0 \\ 0 & 0 & \frac{EA}{l} & 0 & 0 & 0 & 0 & 0 & 0 & 0 \\ 0 & -EI_x\frac{6}{l^2} & 0 & EI_x\frac{4}{l} & 0 & 0 & 0 & 0 & 0 & 0 \\ EI_y\frac{6}{l^2} & 0 & 0 & 0 & EI_y\frac{4}{l} & 0 & 0 & 0 & 0 & 0 \\ 0 & 0 & 0 & 0 & 0 & K_{6,6} & K_{6,7} & 0 & 0 & 0 \\ 0 & 0 & 0 & 0 & 0 & K_{7,6} & K_{7,7} & 0 & 0 & 0 \\ 0 & 0 & 0 & 0 & 0 & 0 & 0 & K_{8,8} & 0 & 0 \\ 0 & 0 & 0 & 0 & 0 & 0 & 0 & 0 & K_{9,9} & K_{9,10} \\ 0 & 0 & 0 & 0 & 0 & 0 & 0 & 0 & K_{10,9} & K_{10,10} \end{bmatrix} \tag{21}$$

3. Curve girder element stiffness analysis

3.1 Restrained torsion stiffness analysis of the thin-walled curve box girder

3.1.1 Local coordinate and the unknown quantity of the displacement

Curve girder element of the thin-walled same cross-section is shown in Fig. 4, geometric center axis of the space flexure is proposed on the same plane, and S_iS_j is an eccentric displacement y_0 between shearing force center and geometric center. To calculate conveniently, authors take no account of factors of the eccentric displacement. Radius of the geometrical center is R_G, and radius of the shear force center is R_s.

Local coordinate system adopts curve line coordinate, z axis directory of the local coordinate points to the tangential direction of the girder axis line, and its directory accords with element directory. X axis lies in curvature plane, the x axis is normal to z axis, and the x axis that points at

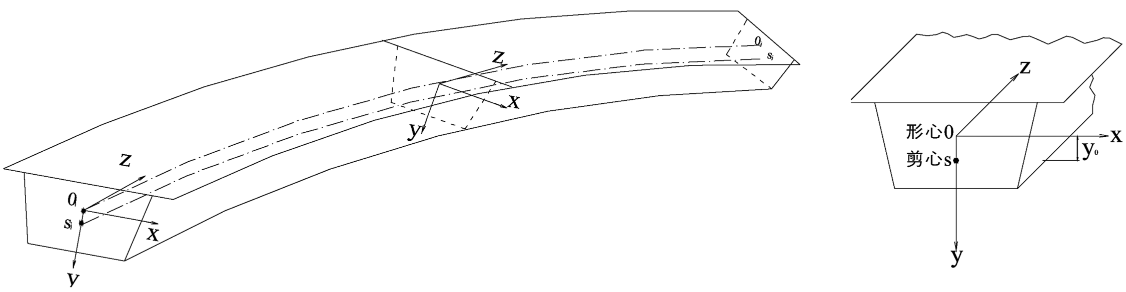

Fig. 4 Spatial curve girder element

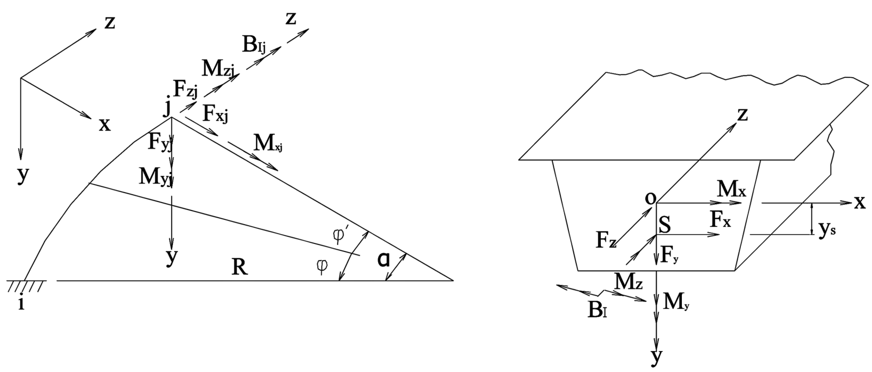

(a) (b)

Fig. 5 Nodal forces of curve girder warping element

right-side of element directory is positive. The local coordinate system conforms to the principle of right hand screw, and it is normal curvature when curvature center lies in the right of element directory and negative in the left. The vectors of the node displacement and bar end force of the curve element accord with the straight girder element.

3.1.2 Strain energy of the curve girder element

Buckling element of curve girder is shown in Fig. 5. According to static structure and balance relation, internal force formulation (22) of each cross-section is acquired except for the buckling bimoment $B(\varphi)$ when j end is put on seven bar end force $F_{xj}, F_{yj}, F_{zj}, M_{xj}, M_{yj}, M_{zj}, B_j$. The buckling bimoment can be presented by the Eq. (22). In the Eq. (22), $I_{\hat{\omega}}$ is a moment of inertia of the cross-section fan shape.

$$\left.\begin{aligned} f'''(\varphi)-k^2f'(\varphi) &= -\frac{\mu}{EI_{\hat{\omega}}}\left(\pm\frac{M_x-F_zy_0}{r}-m_t\right) \\ B(\varphi) &= -EI_{\hat{\omega}}f'(\varphi) \end{aligned}\right\} \tag{22}$$

The strain energy of buckling element of the curve girder in the Fig. 3 has two aspects: taking account of buckling effect and taking no account of buckling effect.

$$U = U_I + U_{II} \tag{23}$$

In the Eq. (23)

$$U_I = \int_l\frac{F_x^2ds}{2GA_{sx}} + \int_l\frac{F_y^2ds}{2GA_{sy}} + \int_l\frac{F_z^2ds}{2EA} + \int_l\frac{M_x^2}{2EI_x}ds + \int_l\frac{M_y^2}{2EI_y}ds + \int_l\frac{M_z^2}{2GK}ds$$

$$U_{II} = \int_l\frac{B^2}{2EI_{\hat{\omega}}}ds + \int_l\frac{B'^2}{2\mu GK}ds - \int_l\frac{M_zB'}{GK}ds$$

3.1.3 Element stiffness matrix

Stiffness matrix of the curve girder element can be acquired through the flexible degree matrix.

1) Space flexible degree subsidiary matrix of the element

Based on castigliano theorem $f_{kl} = (\partial U/\partial F_{lj})_{F_{kj}=1}$, each flexible degree coefficient of the flexible degree subsidiary matrix $[F_{jj}]_{7\times7}$ of the thin-walled curve girder buckling element j end can be acquired.

2) Space stiffness matrix of element

The element of curve girder is similar to the straight girder element, authors adopt matrix form, and the space stiffness matrix is expressed in Eq. (24). The subsidiary matrix $[\vec{K}_{jj}]$ of the Eq. (24) can be presented through the flexible degree matrix based on the relation formulation (25) of between the flexible degree matrix and stiffness matrix.

$$[\overline{K}]^e = \begin{bmatrix} \overline{K}_{ii} & \overline{K}_{ij} \\ \overline{K}_{ji} & \overline{K}_{jj} \end{bmatrix} \tag{24}$$

$$[\overline{K}_{jj}] = [F_{jj}]^{-1} \tag{25}$$

According to the stiffness coefficient definition, it is positive when reactor force of i end accord with normal directory of i end local coordinate. Then the stiffness subsidiary matrix can be presented in Eq. (26). $[R]$ is a reactor force matrix of i end when j end act on the generalized unit force in the Eq. (26). $\overline{K}_{ii}$ can be obtained through the stiffness subsidiary matrix $[\overline{K}_{jj}]$ according to the symmetrical relation between i node and j node, as shown in Eq. (27).

$$\left.\begin{aligned} [\overline{K}_{ii}] &= -[R][\overline{K}_{ij}] \\ [\overline{K}_{ji}] &= [\overline{K}_{ij}]^T \end{aligned}\right\} \tag{26}$$

$$\begin{bmatrix} k_{11} & & & & & & \\ k_{21} & k_{22} & & & & & \\ -k_{31} & -k_{32} & k_{33} & & & & \\ -k_{41} & -k_{42} & k_{43} & k_{44} & & & \\ -k_{51} & -k_{52} & k_{53} & k_{54} & k_{55} & & \\ k_{61} & k_{62} & -k_{63} & -k_{64} & -k_{65} & k_{66} & \\ -k_{71} & -k_{72} & k_{73} & k_{74} & k_{75} & -k_{76} & k_{77} \end{bmatrix}_{jj} \tag{27}$$

3.2 Distortion stiffness analysis of the thin-walled curve box girder

Each stiffness coefficient in the curve girder element distortion stiffness matrix accords with the straight girder.

3.3 Shearing force lag effect stiffness analysis of the thin-walled curve box girder

3.3.1 Overall potential energy function

1) Vertical flexure strain energy

$$\varepsilon_z = \omega_\zeta \zeta'; \quad \gamma_{\bar{x}z} = \frac{\partial \omega \zeta}{\partial \bar{x}} \zeta = h_i \frac{3x^2}{b_i^3} \zeta; \quad \omega_\zeta = -hi\left(1 - \frac{x^3}{b_i^3}\right); \quad \overline{\omega}_\zeta = \frac{\partial \omega}{\partial \bar{x}} = hi\frac{3x^2}{b^3 i}$$

$$\Pi_M = \frac{E}{2}\int_v (\varepsilon_z)^2 d_v = \frac{E}{2}\int_v [\omega_\zeta \zeta'(z)]^2 d_v \tag{30}$$

2) Wing slab shearing lag buckling strain energy

$$\Pi r = \frac{G}{2}\int_v (r_{z\bar{x}})^2 d_v = \frac{G}{2}\int_v \left(\frac{\partial_{\omega\zeta}}{\partial_{\bar{x}}}\zeta\right)^2 d_v = \frac{G}{2}\int_v \bar{\omega}^2 \zeta^2 dv \tag{31}$$

3) External force work under distribute loading and end node force

$$\overline{W} = -\int_l (q_x u + q_y v + q_z w + m_x \theta_x) dz - \{\overline{F}\}^T \{\bar{u}\} \tag{32}$$

In the Eq. (32), the end node force $\{\overline{F}\}$ and the vector $\{\bar{u}\}$ of the element displacement:

$$\{\overline{F}\} = [N_i \ F_{yi} \ M_{xi} \ M_{\zeta}i \ F_{xi} \ M_{yi} \ N_j \ F_{yj} \ M_{xj} \ M_{\zeta j} \ F_{xj} \ M_{yj}]^T$$

$$\{\bar{u}\} = [w_{Gi} \ v_{si} \ \theta_{xi} \ \zeta i \ u_{si} \ \theta_{yi} \ w_{Gj} \ v_{sj} \ \theta_{xj} \ \zeta_j \ u_{sj} \ \theta_{yj}]^T$$

$\{M_{\zeta i}\}$ is a corresponding force factor of the shearing force lag displacement freedom degree ζ. Because of only taking account of the shearing force lag effect, the external work can be expressed as follows (Zhang *et al.* 1998, Luo *et al*. 2004, Wu *et al.* 2004, Nie 2000).

$$\overline{W} = -\{M_{\zeta}i, M_{j\zeta}\}^T \{\zeta_i, \zeta_j\}$$

So, the overall potential energy functions of the curve box girder can be presented as follows

$$\Pi = \Pi_M + \Pi_r + \overline{W} = \frac{E'}{2}\int_v [\omega_\zeta \zeta'(z)]^2 dv + \frac{G}{2}\int_v \bar{\omega}^2{}_\zeta \zeta^2 dv - \{\overline{F}\}^T\{\bar{u}\}$$

$$= \frac{E'}{2}\int_l (I_\zeta \zeta'^2) dz + \frac{G}{2}\int_l (\zeta)^2 K_\zeta dz - \{\overline{F}\}^T\{\bar{u}\} \tag{33}$$

In the Eq. (33):

A: cross-section area, $I_\zeta = \int_A \omega^2{}_\zeta dA$, $K_\zeta = \int_A \bar{\omega}^2{}_\zeta dA$

Then, according to the theorem of virtual work, necessary condition of the system balance state under external force is minimum value of overall potential energy, and the equation formulation (34) is equal zero. At the same time the boundary condition meets the following: $\zeta\rceil_{z=0} = \zeta i$; $\zeta\rceil_{z=0} = \zeta j$.

So, the basic differential equation only taking account of shearing force lag effect can be obtained. In addition, according to the force boundary condition and taking account of shearing lag effect, the corresponding cross-section force factors of the shearing force lag displacement is

$$M_\zeta = E' I_\zeta \zeta'$$

$$\delta\Pi = \delta\left(\int_l \Gamma(\zeta, \zeta')dz\right) = 0 \tag{34}$$

$$-\frac{d}{dz}\left(\frac{\partial\Gamma}{\partial\zeta'}\right) + \frac{\partial\Gamma}{\partial\zeta} = 0 \tag{35}$$

$$GK_\zeta \zeta - E' I_\zeta \zeta'' = 0 \tag{36}$$

3.3.2 Stiffness coefficient

To calculate stiffness coefficient of the element, external force should be put aside, and solution of Eq. (33) can be presented as follows:

$$\zeta(z) = A_1 e^{kz} + A_2 e^{-kz} \tag{37}$$

In the Eq. (37):

$k = \sqrt{GK_\zeta/(E'I_\zeta)}$

A_1, A_2: Integral constant based on boundary condition.

Then according to the order of the Eq. (2) freedom degree, shearing force lag effect deformation stiffness can be expressed as follow

$$\begin{bmatrix} K_{8,8} & K_{8,18} \\ K_{18,8} & K_{18,18} \end{bmatrix} [\zeta i, \zeta j]^T = [M_{\zeta i}, M_{\zeta j}]^T \tag{38}$$

In accordance with the definition of stiffness coefficient, taking account of normal directory regulation of shearing force lag, the stiffness coefficient of the Eq. (38) can be presented

$$K_{8,m} = -E'I_\zeta \zeta'\big|_{z=0}, \quad K_{18,m} = E'I_\zeta \zeta'\big|_{z=l} \tag{39}$$

When each freedom degree brings about unit displacement, the subscript m adopts 8, 18 in turn, that is, when i end ($z = 0$) brings about unit displacement, vectors of others displacement are zero value.

$$\zeta(z=0) = A_1 e^{kz} + A_2 e^{-kz} = 1 \qquad \zeta(z=l) = A_1 e^{kz} + A_2 e^{-kz} = 0$$

$$M_\zeta = E'I_\zeta \frac{k}{1-e^{2kl}}(e^{kz} + e^{2kl} e^{-kz})$$

I end brings about unit displacement but the vectors of other displacement are zero, and the response produced by i end and j end can be presented as follows.

$$K_{8,8} = M_\zeta = -EI_\zeta k/th(kl); \quad K_{8,18} = M_\zeta = -EI_\zeta k/sh(kl)$$

Therefore, authors can obtain stiffness coefficient as follows:

$$K_{18,18} = -EI_\zeta k/th(kl); \quad K_{18,8} = -EI_\zeta k/sh(kl)$$

According to the characteristic of the curve box girder structure and the mechanic behavior, the moment, the torsion and the distortion and the others under external loading couple mutually. In order to simplify analysis and ensure precision, this paper only takes account of interaction between flexure and torsion, and did not takes account of interaction other factors. Therefore, after taking account of the restrained torsionthe distortion anglethe distortion warp and the shearing force lag effect based on elementary girder theory, authors obtain a thin-walled curve box girder analytical element stiffness matrix $[K]_{20\times 20}$ of 10 degrees of freedom of every node. In order to shorten this paper, only the element stiffness matrix $[K_{I,I}]$ is shown in Eq. (40). In the Eq. (40), stiffness matrix coefficient $K_{i,j}$ of shearing force lag effect and the distortion accord with the straight girder, and

$m_{i,j}$ is the flexible degree coefficient. To analyze conveniently, authors use "*m*" form, its value bases on literature (Huang and Xie 2000).

$$\begin{bmatrix} m_{11} & & & & & & & & & \\ m_{21} & m_{22} & & & & & & & & \\ -m_{31} & -m_{32} & m_{33} & & & & & & & \\ -m_{41} & -m_{42} & m_{43} & m_{44} & & & & symmetry & & \\ -m_{51} & -m_{52} & m_{53} & m_{54} & m_{55} & & & & & \\ m_{61} & m_{62} & -m_{63} & -m_{64} & -m_{65} & m_{66} & & & & \\ -m_{71} & -m_{72} & m_{73} & m_{74} & m_{75} & m_{76} & m_{77} & & & \\ 0 & 0 & 0 & 0 & 0 & 0 & 0 & K_{8,8} & & \\ 0 & 0 & 0 & 0 & 0 & 0 & 0 & 0 & K_{9,9} & \\ 0 & 0 & 0 & 0 & 0 & 0 & 0 & 0 & K_{10,9} & K_{10,10} \end{bmatrix} \tag{40}$$

4. Finite element procedure composition based on this paper's theorem

The whole set of thinking of the procedure composition calculation analysis: The structure was divided into space straight girder element and curve girder element based on this paper's theory that is the thin-walled box girder stiffness matrix analysis, and the finite element analytical method is adopted. In addition, the procedure composition adopts FORTRAN language. As for the range of the use of the procedure, boundary-value as well as other noticeable problems have been discussed in the other paper.

5. Analysis of engineering application of Y-shape thin-walled box girder bridge

5.1 Engineering introduction

One Y-shape bridge is shown in Fig. 6, the main string bridge adopts three-span pre-stressed concrete thin-walled continuous box girder, the length of the main string span is composed of 27.5 m + 50 m + 27.5 m, and the width of the bride is 12.6 m. The ramp of the bridge adopts three-span pre-stressed concrete thin-walled continuous curve box girder, the radius of the ramp is 50 m, the span length of the ramp is consist of 31 m + 45 m + 31 m, the width of the bridge is 9.2 m, and design loading adopts Chinese standard Qiche-20.

5.2 Structural static analysis

In order to validate the precision and convenience of this paper's theory, authors analyze the Y-shape bridge structure according to the elementary beam element model, space shell theory model and this paper's theory model analytical method that is the spatial thin-walled box girder element grillage analysis method respectively (Kim *et al.* 2007, Huang 1998, 2002, Wu *et al.* 2004,

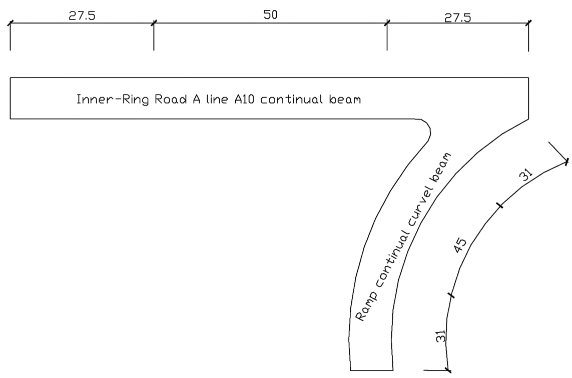

Fig. 6 The simplified version of Y-shape bridge (m)

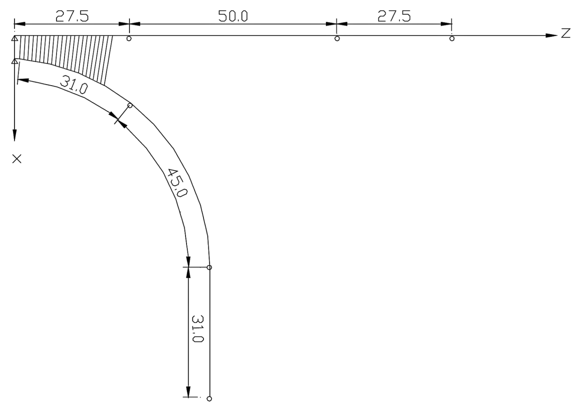

Fig. 7 This paper theoretical model (m)

Table 1 the comparison of the resolute scales of three analytical models

Structure analysis model	Node numbers	Element numbers	Freedom degree numbers
Basic space pole model	203	224	1218
This paper's theory model	203	224	1827
Space shell structure model	4471	4319	17884

O'Briven and Keogh 1998, Hao 2005). The analytical calculating scales of the three different theories above are obtained, as shown in Table 1. The spatial thin-walled box girder element grillage analysis calculation model was built based on this paper's theorem, as shown in Fig. 7.

5.3 Comparison of theory analysis results with experimental test

The Y-shape bridge structure analysis adopts three kinds of theories and two kinds of loading cases. The first loading cases: three 300 kN standard loadings were collocated symmetrically only on the middle location of the main string 50 m span. The biggest moment of the middle location of the 50 m span of the main string was obtained. The second loading cases: two 300 kN standard loadings were collocated symmetrically only on the middle location of 45 m span of the bridge ramp curve girder. The biggest normal moment of the middle location of the 45 m ramp curve girder was obtained. In order to shorten the length of the paper, authors just give out a portion of the analytical results.

5.3.1 Deflection contrast

Deflection contrast under the second loading cases is shown in Fig. 8. According to Fig. 8, the results of elementary beam element model calculation have great deviation, the results of the shell model is most close to the results of the experimental test, the results of this paper's theorem that is the spatial thin-walled box girder element grillage analysis model is close to the results of the shell model and experimental test.

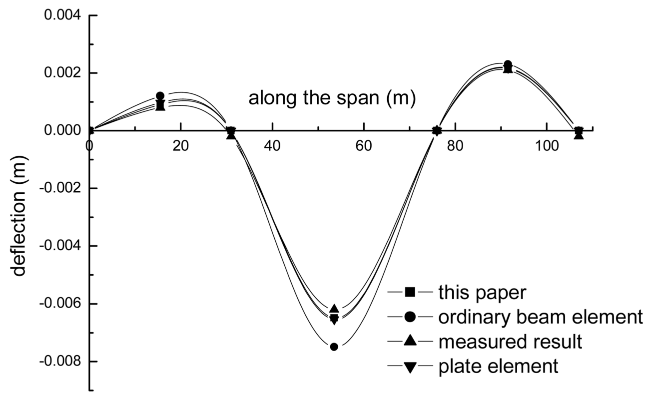

Fig. 8 The deflection comparison of ramp under the second loading cases

5.3.2 Strain contrast

Strain contrast under the first loading cases is shown in Table 2.

Table 2 the strain comparison of sections under the first loading cases (Unit: 10^{-6})

Section	Strain measure node	Basic beam element	Shell element	Theory results of this paper	Measure results
A-A	1	34.5	15.7	31.1	18
	2	34.5	15.4	28.6	—
	3	34.5	14.8	26.1	19
	4	-36.3	-40.6	-37.9	-38
	5	-36.3	-40	-36.5	-39
	6	-36.3	-39.2	-35.0	-38

Notice: A-A section is the middle location of the main string span.

6. Conclusions

The mechanical behavior of the Y-shape thin-walled box girder bridge structure is complex, so one can not exactly hold the mechanical behavior of the Y-shape thin-walled box girder bridge structure through general calculation theory and analytical method. To hold the mechanical behavior better, based on elementary beam theory, by increasing degree of freedom of the analytical method, taking account of the restrained torsionthe distortion anglethe distortion warp and the shearing lag effect, authors obtained a thin-walled box beam analytical element of 10 degrees of freedom of every node, derive stiffness matrix of the element, and code a finite element procedure.

Authors analyze a typical Y-shape thin-walled box girder bridge structure according to the elementary beam theory analytical method, the shell theory analytical method and the spatial thin-walled box girder element grillage analysis method respectively. The comparisons of results of theory analysis with experimental text show that the spatial thin-walled box girder element grillage analysis method is of accuracy and validity. Meanwhile, it indicates that the analytical method of the spatial thin-walled box girder element grillage can simulate the complex the Y-shape bridge structure as a spatial grillage system of intersection relation. The mechanic model of the spatial grillage system conforms to the cases of the practical mechanic structure, one can obtain directly the structural internal force and deformation. The research results are helpful for mechanic property of these Y-shape thin-walled box Girder bridge structures

Acknowledgements

This program is funded by the construction committee of Guangzhou Province, China.

References

Ding, H.S. and Shao, R.G. (1996), "Analysis of plan abnormity bridge", The Twelfth China Bridge Science Conference.

Hambly, E.C. (1982), "Bridge super structural capability", Beijing: China Communication Press.

Hao, W.H. (2005), "ANSYS civil engineering application example", Beijing, China Water Electricity Press.

Huang, H.Y. (2002), "Y-shape bridge mechanic analysis take account of constrained torsion, distortion effect", Guangzhou: Huanan Science and Technology University.

Huang, J.Y. (1998), "Turn back analysis of thin-walled structure", Beijing, China Railway Press.

Huang, J.Y. and Xie, X. (1994), "Stiffness method of thin-walled curve pole structure analysis", *J. Civil Eng.*, **5**, 3-19.

Huang, J.Y. and Xie, X. (2000), "Structure theory and calculation method of the viaduct bridge", Beijing, Science Press.

Kim, N.I., Fu, C.C. and Kim, M.Y. (2007), "Stiffness matrices for exural-torsional/lateral buckling and vibration analysis of thin-walled beam", *J. Sound Vib.,* **299**, 739-756.

Li, P. and Cong, Y.S. (1996), "Box beam bridge design of Y-shape compose structure", *High-way*, **11**, 29-31.

Luo, Q.Z., Tang, J., Li, Q.S., Liu, G.D. and Wu, J.R. (2004), "Membrane forces acting on thin-walled box girders considering shear lag effect", *Thin Wall. Struct.*, **42**, 741-757.

Mira Mitra, S., Gopalakrishnan, M. and Seetharama Bhat. (2004), "A new super convergent thin walled composite beam element for analysis of box beam structures", *Int. J. Solids Struct.,* **41**, 1491-1518.

Morreu, P.J.B., Riddington, J.R., Ali, F.A. and Hamid, H.A. (1996), "Influence of Joint Detail on the Flexural/ Torsional Interaction of Thin-Walled Structures", *Thin Wall. Struct.*, **24**, 97-111.

Nie, Y.Z. (2000), "Analysis of elastic thin-walled beam bridge", Beijing: China Communication Press.

O'Briven, E.J. and Keogh, D.L. (1998), "Up stand finite element analysis of slab ridges", *Comput. Struct.*, **69**, 671-683.

Thuc Phuong Vo and Lee, J.H. (2006), "Flexural-torsional behavior of thin-walled closed-section composite box beams", *Eng. Struct.*, **29**(8), 1774-1782.

Wu, S.X., Chen, H.P. and Huang, J.Y. (1996), "Box girder bridge analysis with irregular arbitrary play geometry", *J. Ninbo University*, **3**, 126-134.

Wu, Y.P., Yu, S.S., Shi, C.H., Li, J.J., Lai, Y.M. and Zhu, Y.L. (2004), "Ultimate load analysis of thin-walled box beams considering shear lag effect", *Thin Wall. Struct.*, **42**, 1199-1210.

Yaping Wu, Yuanming Lai, Xuefu Zhang and Yuanlin Zhu. (2004), "A finite beam element for analyzing shear lag and shear deformation effects in composite-laminated box girders", *Comput. Struct.,* **82**, 763-771.

Zhang, S.D., Deng, X.H. and Wang, W.Z. (1998), "Thin-walled box beam shear lag effect", Beijing, China Communication Press.